Structure of deposits formed by drying of droplets contaminated with Bacillus spores determines their resistance to rinsing and cleaning

Maureen Deleplace, Heni Dallagi, Thomas Dubois, Elodie Richard, Anna Ipatova, Thierry Bénézech, Christine Faille

▶ **To cite this version:**

Maureen Deleplace, Heni Dallagi, Thomas Dubois, Elodie Richard, Anna Ipatova, et al.. Structure of deposits formed by drying of droplets contaminated with Bacillus spores determines their resistance to rinsing and cleaning. Journal of Food Engineering, 2022, 318, pp.110873. ⟨10.1016/j.jfoodeng.2021.110873⟩. ⟨hal-03754070⟩

HAL Id: hal-03754070

https://hal.science/hal-03754070v1

Submitted on 19 Aug 2022

HAL is a multi-disciplinary open access archive for the deposit and dissemination of scientific research documents, whether they are published or not. The documents may come from teaching and research institutions in France or abroad, or from public or private research centers.

L'archive ouverte pluridisciplinaire **HAL**, est destinée au dépôt et à la diffusion de documents scientifiques de niveau recherche, publiés ou non, émanant des établissements d'enseignement et de recherche français ou étrangers, des laboratoires publics ou privés.

Distributed under a Creative Commons CC BY-NC-ND 4.0 - Attribution - Non-commercial use - No Derivative Works - International License

Journal of Food Engineering 318 (2022) 110873

Contents lists available at ScienceDirect

Journal of Food Engineering

journal homepage: www.elsevier.com/locate/jfoodeng

Structure of deposits formed by drying of droplets contaminated with *Bacillus* spores determines their resistance to rinsing and cleaning

Maureen Deleplace [a], Heni Dallagi [a], Thomas Dubois [a], Elodie Richard [b], Anna Ipatova [c], Thierry Bénézech [a], Christine Faille [a,*]

[a] Univ. Lille, CNRS, INRAE, ENSCL, UMET, F-59650, Villeneuve d'Ascq, France
[b] Univ. Lille, CNRS, INSERM, CHU Lille, Institut Pasteur de Lille, US 41 - UMS 2014 - PLBS, F-59000, Lille, France
[c] Univ. Lille, CNRS, UMR 8520 - IEMN, F-59000, Lille, France

ARTICLE INFO

Keywords:
Droplet evaporation
Bacillus spores
Deposition patterns
Material
Hydrophobicity
Surface hygiene

ABSTRACT

The formation of deposits by evaporation of droplets contaminated by *Bacillus* spores was investigated, focusing on the role of spore and material properties. Droplets containing hydrophilic to hydrophobic spores were deposited on materials (stainless steels, polypropylene, glass). The presence of spores within the droplets, as well as material hydrophobicity plays a major role in the kinetics of the droplet shape during drying while the pattern of the dried deposit was affected by both material and spore properties. The resistance to detachment of the different deposits was then investigated. After a single rinsing procedure, a very high resistance to detachment of adherent spores was observed (up to 90% of residual spores). The hydrophilic Bs PY79 spores were the least resistant to removal, while the differences between materials were not pronounced. The ease of cleaning of the dried deposits was much greater. The least resistant spores were still the Bs PY79 ones, while the detachment was 3–100 times more effective on glass than on other materials.

These results highlight the predominant role of hydrophilic/hydrophobic properties of particles and materials on the structure of deposits and their further resistance to rinsing and cleaning procedures.

1. Introduction

In food industries, contamination of equipment surfaces is of concern, as contaminated surfaces can serve as a source of cross-contamination in foods, therefore compromising food quality and safety (Coughlan et al., 2016) and resulting in the rejection of the products, economic losses and even diseases if food-borne pathogens are involved. A source of surface contamination is the presence of bio-aerosols (aerosols containing particles of biological origins) that settle on surfaces and equipment and thus contribute to the food contamination during food preparation and packaging. Indeed, it has long been known that many micro-organisms are present in aerosols in food environments. This is the case, for example, with yeasts in fruit juice production units, molds in cake factories or wheat or rice flour mills, or bacteria in milk processing plants or slaughterhouses (Theisinger and Smidt, 2017).

These bioaerosols can come from ventilation systems and evaporators, as air currents are known to be important vectors for the spread of potentially pathogenic organisms (Eduard et al., 2012). They can also be formed during certain operations during food processing, such as washing fruits and vegetables (high pressure water systems, "bubbling" in tanks with the production of air bubbles). Furthermore, they are also often associated with rinsing or cleaning operations e.g. high pressure cleaning of drains or floors (Faille and Billet, 2020), which causes the dispersion of water droplets over distances sometimes exceeding 2 m in height and 5 m in length (Holah, 2018). One of the major problems posed by these bioaerosols is that some harmful bacteria are able to survive inside droplets or even resist further desiccation. Indeed, it has been shown that *L. monocytogenes*, a non-sporulating bacterium, can survive more than 3 h in aerosols (Spurlock and Zottola, 1991). Furthermore, some food-borne pathogens such as *Salmonella typhimurium* or *L. monocytogenes* and of course bacterial spores, such as *Bacillus* spores, resist a period of desiccation quite well, especially in the presence of food residues (Kuda et al., 2015).

When droplets are deposited on a surface and subjected to a drying step, this will result in the formation of a deposit whose structure is

* Corresponding author. INRAE, UMET, 369 rue Jules Guesde, F-59650, Villeneuve d'Ascq, France.
E-mail address: christine.faille@inrae.fr (C. Faille).

https://doi.org/10.1016/j.jfoodeng.2021.110873
Received 19 July 2021; Received in revised form 29 October 2021; Accepted 31 October 2021
Available online 12 November 2021
0260-8774/© 2021 The Author(s). Published by Elsevier Ltd. This is an open access article under the CC BY-NC-ND license (http://creativecommons.org/licenses/by-nc-nd/4.0/).

affected by the properties of particles inside (Burkhart et al., 2017; Devlin et al., 2015; Yunker et al., 2011). As for all interfacial phenomena, material wettability (Baughman et al., 2010) and topography (Susarrey-Arce et al., 2016) also play a crucial role both in the spread of the droplet, as well as in the size and organization of the deposit obtained after its total evaporation. For example, the evaporation-driven patterns can take the form of a ring-like deposit (coffee-ring pattern), or of multi-rings, uniform deposits or even combined structures. Depending on the form this deposit will take (i.e. in the form of isolated cells or of a thick deposit), it can be assumed that this will affect the effectiveness of the procedures implemented to control surface hygiene.

This work was designed to investigate the potential role of the surface hydrophobicity of materials and of spores contained within droplets on phenomena occurring during evaporation of contaminated droplets settled on materials and on the resulting deposit after complete drying. We also explored the consequences of the deposit patterns on their ease of removal, using a rinsing or cleaning procedure.

2. Material & methods

2.1. Material

Five *Bacillus* strains were used throughout this study. *B. cereus* CUETM 98/4 (subsequently named Bc 98/4) was isolated from a dairy processing line, *B. cereus* D6 (Bc D6) from a patient with diarrheic symptoms following ingestion of contaminated foods. *B. subtilis* PY79 (Bs PY79) is a laboratory strain. *B. cereus* strains are surrounded by a soft membrane, called exosporium, and appendages, while *B. subtilis* spores are surrounded by a mucous layer called crust. Two Bs PY79 recombinant strains, modified in their surface properties (crust composition) and characterized by different surface hydrophobicity, were also used in this study. The *B. subtilis* PY79 *ΔspsA* (Bs PY79 spsA) strain has been described previously (Dubois et al., 2020). The *B. subtilis* PY79 *spsI::erm* (Bs PY79 *spsI*) was constructed as follows: an internal fragment of the *spsI* gene was amplified by PCR using the PY79 chromosomal DNA as template and primers 5′- CCCAAGCTTAACGAAAGCCGTCAACAAG -3’/5′-CGGGATCCATAAGACAGCCCATCCGA-3’. The resulting fragment was purified as a *HindIII-BamHI* fragment and was inserted between the *HindIII* and *BamHI* sites of pMUTIN4. The insert sequence was verified by Sanger sequencing (Eurofins Genomics Germany GmbH) and the plasmid was transformed into the Bs PY79 strain, as previously described (Radeck et al., 2013). The chromosomal recombination was verified by PCR using the chromosomal DNA of the recombinant strain and primers 5′-GCATGAGCTTTGTAAACGTGA-3’/5′-TGACTCTCTAGC TTGAGGCATC-3′ and 5′-GACTGCCGCAATATCCTTG-3’/5′-GTCAGTAA CTTCCACAGTAGTTCA-3’.

The intrinsic fluorescence of the *Bacillus* spores tested in this study allows direct observations under an epifluorescence microscope, without staining. However, to facilitate time-lapse imaging (see section 2.3), Bc 98/4 (Faille et al., 2014) and Bs PY79 (Richard et al., 2020) were tagged with green fluorescent proteins to make the spores more fluorescent.

Spores were produced on Spo8-agar at 30 °C (Faille et al., 2019). After a 10-day incubation period and when the sporulation rate had reached at least 95%, they were harvested by scraping the surface, washed five times in sterile water and stored in sterile water at 4 °C until use. Before each experiment, suspensions were subjected to an ultrasonication step to limit the presence of spore aggregates.

The four materials tested in this study were used in the form of rigid rectangular coupons of 15 mm × 45 mm and of 26 mm × 76 mm. Stainless steel coupons (1 mm thickness) of AISI (American Iron and Steel Institute, Washington, USA) 316 were supplied by APERAM with pickled (SS-2B) and bright annealed (SS-2R) finishes. Polypropylene (PP, 2 mm thickness) was supplied by API Plastiques (Seclin, France) and glass (1 mm thickness) by Glasatelier SAILLART (Meerhout, Belgium). Before each experiment, the materials were subjected to a cleaning and disinfection procedure. The cleaning step consisted of 10 min cleaning by immersion in a 5% alkaline detergent (RBS T105, Traitements Chimiques des Surfaces, France), in softened water (no calcium) at an initial temperature of 60 °C, followed by rinsing in partially softened water (60 ppm $CaCO_3$), then in softened water. 24 h before experiments, stainless steel and glass coupons were sterilized at 180 °C for 1 h in a dry heat oven. The PP coupons were sterilized at 121 °C for 30 min in an autoclave (moist heat).

2.2. Characterization of the spore surface properties

The hydrophobicity of spores was characterized using a partitioning method, based on the affinity of spores to an apolar solvent, hexadecane (Sigma), as previously described (Faille et al., 2019). Three milliliter aliquots of the suspensions and 500 μL of hexadecane were vortexed for times ranging from 5 s to 30 min and left to settle for 30 min to allow complete separation of the two phases. The more hydrophobic the spores, the greater their affinity to hexadecane, thereby resulting in a decrease in the absorbance (A) of the aqueous phase with the vortexing time. $[A_t/A_0]$ was plotted against the vortexing time (s). The hydrophilic/hydrophobic character was evaluated using the initial slope, giving the initial removal rate (R_0) from the aqueous suspension. A particle is considered to be hydrophilic when $-R_0$ falls below 1.0 s^{-1}, moderately for values between 1.0 and 2.0 s^{-1}, and highly hydrophobic for values greater than 2.0 s^{-1}.

2.3. Kinetics of evaporation (dynamic of droplet shapes)

1 μl water droplets containing $\pm 10^8$/mL spores were placed on the different materials and evaporated at room temperature. The shape of the droplets was viewed from the side throughout the drying process, using a goniometer (Digidrop, GBX, France). Photos were taken every 30 s.

In order to follow the possible movements of spores within the droplets during the desiccation step, observations were carried out at the material surface with an inverted confocal laser scanning microscope (Zeiss, LSM780). These experiments were performed on two transparent materials, hydrophilic glass and hydrophobic glass bottom Petri dishes (MatTek, Ashland, USA). Images were acquired every 5 s with Zen Software with the 488 nm laser line (10x NA 0.45, zoom 0.6).

2.4. Resistance of dried droplets to rinsing and cleaning

In a first set of experiments, the amount of spores placed on the coupons was controlled. Dried deposits were sampled using a dry cotton swab (Copan, Brescia, Italy). The swab was then placed in tubes containing 5 mL of sterile water and then vortexed for 25 s at 2400 rpm. The detached spores were enumerated on Trypton Soy Agar (TSA) after 48 h at 30 °C. In order to ensure the relevance of this method of quantification (efficiency of detachment of adherent spores, no trapping in the swab), preliminary tests were carried out on calibrated spore deposits having undergone the same drying procedure on the different materials. Other coupons were observed either with an inverted confocal laser scanning microscope (Zeiss, LSM780) at a x100 magnification or by epifluorescence microscopy (Zeiss Axoscop 2 plus) at a x50 magnification, to determine the deposit patterns.

In order to estimate the resistance of the dried deposits to a rinsing procedure (mechanical forces), contaminated coupons (26 mm × 76 mm) were inserted into a parallel-plate flow chamber designed and engineered in the laboratory (Faille et al., 2013), with a rectangular flow channel (60-mm length by 4-mm width and 0.5-mm height) and subjected to a wall shear stress of 440 Pa (Delplace, 2018) for 1 min. This wall shear stress, much higher than those encountered in processing and cleaning in the food industry, was chosen to allow the observation of a significant detachment of adherent spores. The flow chamber was then

dismantled and the residual adhering spores were enumerated or observed by epifluorescence microscopy (Zeiss Axoscop 2 plus) at a x50 magnification.

In order to determine the resistance to cleaning of dried droplets, three droplets of 1 μl were placed on coupons (15 mm × 45 mm) which were then maintained at 30 °C for 1 h until completely dry. They were directly analyzed (as above) or placed in rectangular test tubes, connected to a CIP pilot rig (Jullien et al., 2008) and subjected to the following CIP procedure: (i) rinsing for 5 min with softened water at 20 °C at a wall shear stress of 1.34 Pa, (ii) cleaning for 10 min with 0.5% NaOH water at 60 °C at a wall shear stress of 3.60 Pa, and finally (iii) rinsing with softened water at 20 °C at a wall shear stress of 1.34 Pa. After cleaning, the rig was dismantled and 3 coupons were used to evaluate the amount of residual spores after cleaning, as described above. The last coupon was observed under microscope.

2.5. Statistical analysis

The statistical analyses were performed using SAS V9.4 software (SAS Institute, Gary, NC, USA). Each experiment was repeated three or four times. Variance analyses and Tukey's grouping (Alpha level = 0.05) were performed to determine the respective role of bacterial strains and materials on bacterial detachment (in terms of CFU) by a rinsing or a cleaning procedure.

3. Results

3.1. Hydrophilic/hydrophobic property of the spore surface

The hydrophilic/hydrophobic property of the spores was estimated by the affinities of spores to an apolar solvent, hexadecane. As shown in Table 1 andFigure S1 the initial removal rate R_0 efficiently discriminated between spores ($p = 0.0015$) and showed the highly hydrophilic character of the Bs PY79 spores (Tukey' group = B). Among the other strains, the values of the original slope showed that the Bc D6 and Bs PY79 *spsI* spores were strongly hydrophobic (Tukey' group = A), the other spores (Bc 98/4 and Bs PY79 spsA) being moderately hydrophobic (Tukey' group = AB).

Table 1
Character hydrophilic/hydrophobic estimated by the initial removal rate (R0) and properties of the droplets (1 μl) contaminated or not by the spores and deposited on the different materials (initial diameter and water contact angle).

	Water	Bc 98/4	Bc D6	Bs PY79	Bs PY79 spsA	Bs PY79 *spsI*
		Spores surrounded by a flexible layer [exosporium]		Spores surrounded by amucous layer [crust]		
-R0						
Average value	–	2.05	2.80	0.02	1.79	3.63
Tukey's grouping[a]	–	AB	A	B	AB	A
Initial diameter (mm)						
Glass	2.4± 0.0	2.1± 0.0	2.0± 0.1	2.1± 0.0	2.0± 0.1	2.0± 0.0
SS-2R	2.3± 0.1	1.9± 0.0	1.7± 0.1	2.0± 0.1	1.8± 0.1	1.8± 0.0
SS-2B	2.3± 0.0	1.8± 0.1	1.6± 0.1	1.9± 0.1	1.7± 0.1	1.5± 0.1
PP	1.5± 0.1	1.3± 0.1	1.3± 0.3	1.3± 0.1	1.3± 0.0	1.3± 0.0
Initial water contact angle						
Glass	40.6° ±0.6	46.6° ±1.0	51.0° ±4.5	49.6° ±0.0	48.1° ±2.0	48.0± 0.0
SS-2R	41.6° ±0.1	56.7° ±1.2	67.4° ±0.5	54.3° ±2.5	63.2° ±3.7	62.0° ±1.2
SS-2B	49.9° ±2.6	64.8° ±0.1	75.5° ±6.9	59.7° ±1.7	69.8° ±3.0	82.8° ±4.4
PP	106.4° ±0.3	101.5° ±1.1	99.6° ±3.0	97.6° ±2.0	97.8° ±1.3	91.6° ±1.9

[a] Tukey's grouping (groups in the same column with common letters are not significantly different).

3.2. Evolution of the shape of the droplets during the evaporation process

The shape of the 1 μl droplets (with or without *Bacillus* spores) during the evaporation process was monitored via a goniometer (Fig. 1, Table 1). First, clear differences were observed between the four materials: the initial droplet diameter was the greatest on the glass (hydrophilic), the smallest on PP (hydrophobic). During the first step of evaporation, the droplet diameters generally remained stable, while the height of the droplets decreased. In the second step, the contact lines (or triple lines) receded either steadily or not. This decrease in diameter occurs rapidly on PP, but only in the final drying phase on the other materials, except perhaps in the presence of hydrophilic spores of Bs PY79 (on SS-2R and glass). Lastly, the addition of spores in the droplets seems to limit their spreading on the different materials: the diameter was smaller, the contact angle larger in the presence of spores, whatever their surface properties.

3.3. Deposition patterns of spores after droplet evaporation

Different deposition patterns after complete evaporation (±11 min on glass and stainless steels; ±25 min on PP) were observed by confocal microscopy (Fig. 2). Whatever the spores contained in the droplets, the widest deposits were observed on the hydrophilic glass, the smallest deposits on the hydrophobic PP. On the other hand, no clear trend appears from the images in Fig. 2 on a possible role of the topography of the materials. Elsewhere, a regular external ring was clearly observed on most deposits, often close to the initial contact line, which would result from a pinning of the droplet during a large part of the drying process. When droplets contained the hydrophilic Bs PY79 spores, the ring was regular and thick, with relatively few spores adhered within the ring. However, on glass, in addition to the peripheral ring shape, several rings were sometimes observed, probably due to successive steps of fixation and sudden release of the contact line. For the more hydrophobic spores, in addition to the more or less clear outer ring, a diffuse peripheral deposit was often observed. Thus, the outermost part of most deposits was often more heavily contaminated than the middle area. Many spore clusters were observed on the deposits formed by both *B. cereus* spores and these clusters were observed across the whole surface, probably because these clusters adhered strongly to the different materials. As such clusters were not observed for the hydrophobic to very hydrophobic Bs PY79 spsA and *spsI* spores, it is likely that the presence of an exosporium surrounding the *B. cereus* spores was responsible for their formation.

3.4. Phenomena occurring during evaporation

The movement of spores during the evaporation of droplets on hydrophilic and hydrophobic (glass bottom Petri dish) glass is shown in videos in supplementary data. As can be seen clearly in the video of the Bc 98/4 spores on the hydrophobic glass (Video S1), only few large clusters (some of which continue to be deposited during the drying process) moved during evaporation, probably because they strongly interact with the material, while many single spores and small spore clusters migrated to the outside of the droplet. On the hydrophilic glass (Video S2), more spores and spore clusters were subjected to the outward motion and their movement was faster, probably due to weaker interactions between the spores and the material. However, at the end of the drying process on both materials, as the droplet decreases in diameter, the spores were not subjected to centripetal movement, again probably due to a strong interaction between the spores and the

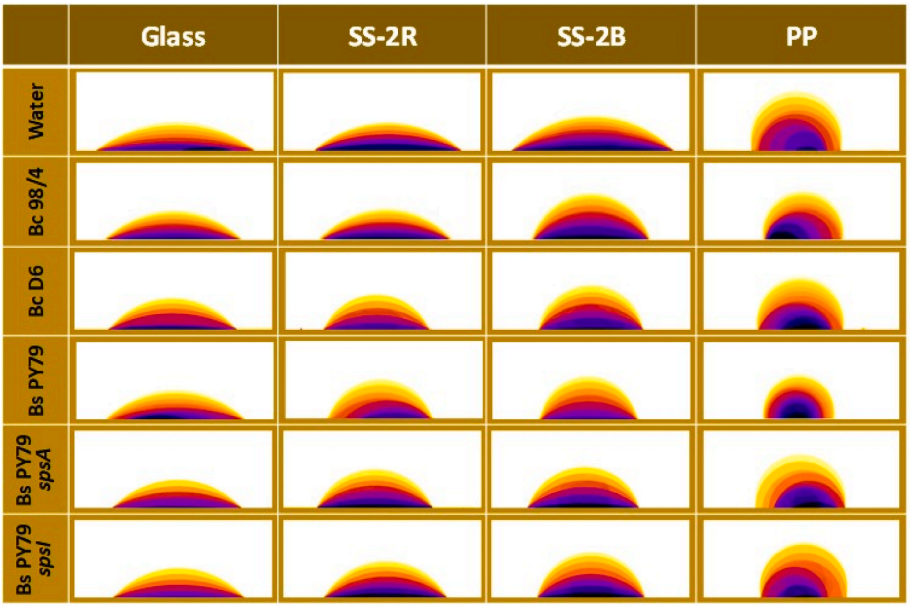

Fig. 1. Evolution of the shape of the droplets during the evaporation process on the different materials. The colour code ranges from yellow (T0) to black (dried droplet). (For interpretation of the references to colour in this figure legend, the reader is referred to the Web version of this article.)

material.

Supplementary data related to this article can be found at https://doi.org/10.1016/j.jfoodeng.2021.110873.

With Bs PY79 spores, no cluster could be observed at any stage of drying on both materials. On the hydrophobic glass (Video S3), the diameter of the droplets decreased with time and the spores were thus probably subjected to both centripetal and centrifugal forces, which may explain the difficulty in observing a clear trend in the spore direction during drying. Lastly, on the hydrophilic glass (Video S4), after a short period with irregular trajectories, rapid outward motions were observed, which initially concerned the outermost zones of the droplet, then the more and more inner zones. At the end of the drying process, contrary to what was observed for Bc 98/4 spores, Bs 98/7 spores were subjected to a centripetal movement that concerned all spores on the hydrophobic material, but only some of them on the hydrophilic material.

Supplementary data related to this article can be found at https://doi.org/10.1016/j.jfoodeng.2021.110873.

3.5. Resistance of the dried droplets to a rinsing procedure

The contaminated coupons were subjected to a rinsing procedure to determine the resistance of the different deposits to the mechanical action generated by the water flow. As shown in Fig. 3A, the dried deposits were highly resistant to rinsing, with between 28% and 91% residual spores, except for the hydrophilic Bs PY79 spores (around 5% on SS-2R, glass and PP). Finally, the differences between materials are not very marked, except perhaps for the Bs PY79 spores, which are highly resistant to rinsing on SS-2B. The variance analysis confirmed that the amount of residual spores was significantly affected by the strain ($p < 0.0001$) and to a lesser extent to the material ($p = 0.0017$). The Tukey's grouping (Table 2) showed that Bs PY79 was the least resistant strain, while SS-2B was the least cleanable material.

The comparison of Figures S2 and S3, which show epifluorescence microscopy images of dried deposits (Figure S2) and images of deposits subjected to a rinsing procedure in the flow cell (Figure S3), confirmed that spore deposits were difficult to remove in a single rinsing step. Indeed, a large amount of spores were still visible after the detachment step, whatever the stain or material. Only the outer coffee ring was often only faintly or no longer visible after rinsing. Elsewhere, the spores of the different *Bacillus* strains did not react in the same way to this detachment procedure, probably because of their surface properties: the very hydrophilic Bs PY79 spores seem to resist much less than the other spores, being moderately to strongly hydrophobic.

3.6. Resistance of the dried droplets to a cleaning-in-place procedure

The deposits were then subjected to a standard CIP procedure in a pilot rig to determine their resistance to cleaning. The percentages of residual cultivable cells after CIP on the different surfaces are presented in Fig. 3B. Great differences were observed in the resistance of spores to the CIP procedure, with less than 0.1% residual adherent spores for Bc 98/4, Bs PY79 and Bs PY79 spsA on glass, and over 50% residual adherent spores for Bc D6 on PP. Elsewhere, Bs PY79 *spsI* spores were highly resistant to detachment whatever the material, contrarily to the other strains (whether surrounded by an exosporium or a crust). In contrast, the hydrophilic Bs PY79 spores were the most easily removed from the four tested materials. The variance analysis confirmed that the amount of residual spores was significantly affected both by the strain ($p < 0.0001$) and the material ($p < 0.0001$). The Tukey's grouping (Table 2) showed that the most resistant strain was Bs PY79 *spsI* and the least resistant one was Bs PY79. Concerning the material, the Tukey's grouping indicated that the dried droplets contaminated with *Bacillus* spores were easily cleaned on glass, yet much more difficult to remove from polypropylene.

In order to determine whether the different areas of the spore deposits were more or less easily removed during the cleaning procedure, the coupons were observed by epifluorescence at a x50 magnification after cleaning. The comparison of Figures S2 and S4 clearly indicated that spore deposits resulting from droplet evaporation were relatively difficult to clean, especially on PP and SS-2B. In agreement with the enumeration results, the observations also indicated that Bs PY79 spores were easily removed and that the amount of residual spores was high on PP and very low on glass, on which it was difficult to observe a residual deposit by microscopy. In addition, it is noteworthy that the outer ring was difficult to observe after CIP, although the spore clusters are often still at least partially present.

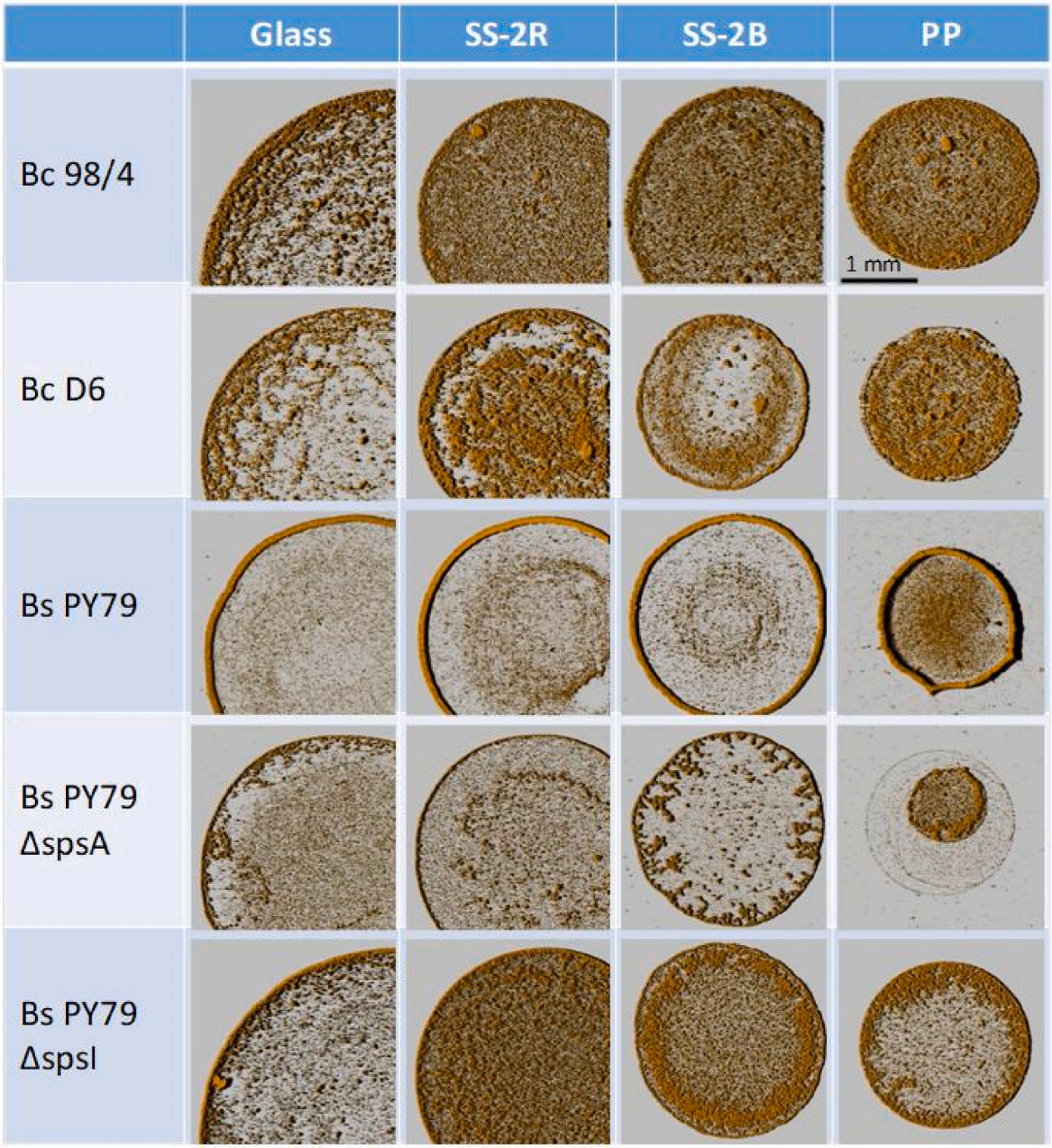

Fig. 2. Deposition patterns of *Bacillus* spores on the four materials, examined by confocal laser scanning microscope (Zeiss, LSM780).

4. Discussion

Due to their frequency in food environments, but also to their high resistance to adverse environmental conditions, such as desiccation or surface hygiene procedures, bacterial spores are probably largely dispersed within bioaerosols and may survive once settled on a surface. For illustration, in the USA, spores belonging to the *B. cereus* group spores have been found to be often present in urban aerosols all year round (Merrill et al., 2006). Indeed, eight of the 11 tested cities were positive for *Bacillus* species in at least 50% of the samples.

Bacillus spores were thus chosen as the biological particles in this study because of their relevance in food environments and of their stable surface properties. Moreover, depending on the *Bacillus* species and even the strain, the spores display quite different surface structures (e.g. presence of an external layer called exosporium on spores belonging to the *B. cereus* group, or of a mucous layer called crust on spores belonging to the *B. subtilis* species and others) resulting in various physicochemical properties.

The deposits formed by the droplets after complete evaporation can have very different patterns depending on the properties of the environment such as humidity, temperature, and receiving material but also on the properties of the particles. Indeed, once the aerosols have settled on a surface, various evaporation modes can be encountered (Fig. 4) and are notably characterized by the pinning (when the contact line is anchored) and depinning properties of the droplet contact line (Parsa et al., 2018). These contact-line dynamics are crucial in determining the deposition patterns of evaporating colloidal droplets. Among these different modes, one can mention the constant contact radius mode (CCR), in which the droplet radius remains constant (stationary contact line), while the contact angle decreases and the constant contact angle mode (CCA), in which the contact angle remains constant (constant droplet shape), while the droplet diameter decreases. Between these two cases, there are numerous documented cases which do not fit into either description, in other words “mixed” modes, where both the contact

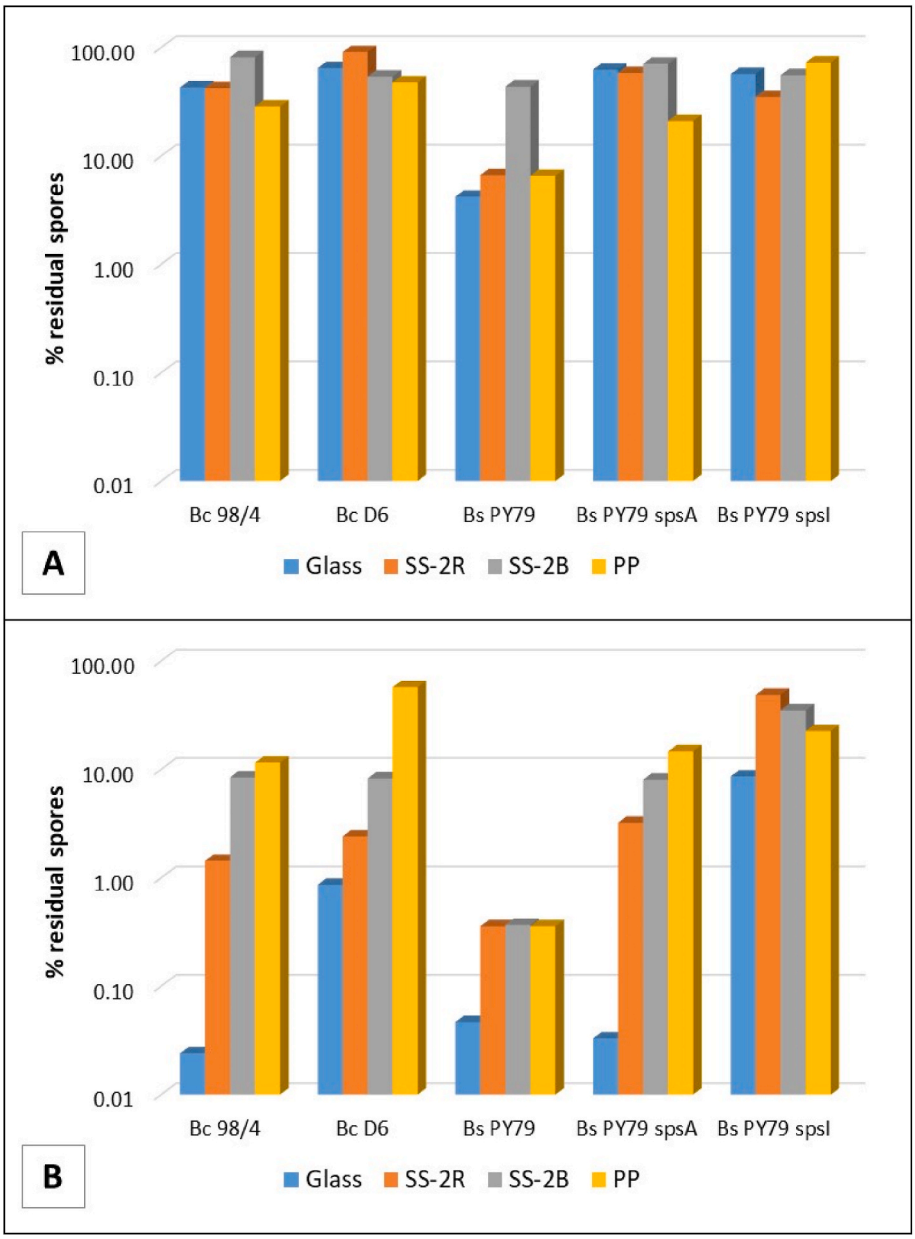

Fig. 3. Percentages of residual cultivable spores on the residual patterns obtained after drying of the contaminated droplets, after a rinsing procedure (A) or a cleaning procedure (B).

Table 2
Influence of *Bacillus* strain and material on the percentage of residual adherent spores (mean values) after detachment.

Strain	Residual Adherent spores (log%)	Tukey's Grouping[a]				Material	Residual adherent spores (log%)	Tukey's Grouping[a]			
Resistance to rinsing											
Bc 98/4	1.61	A				Stainless steel 2R	1.51		B		
Bc D6	1.78	A				Stainless steel 2B	1.76	A			
Bs PY79	0.97		B			Glass	1.49		B		
Bs PY79 spsA	1.67	A				Polypropylene	1.42		B		
Bs PY79 *spsI*	1.72	A				–	–				
Resistance to CIP											
Bc 98/4	0.72			C		Stainless steel 2R	0.37		B		
Bc D6	0.67		B			Stainless steel 2B	0.70	A	B		
Bs PY79	−0.73				D	Glass	−0.73				C
Bs PY79 spsA	0.21		B	C		Polypropylene	0.92	A			
Bs PY79 *spsI*	1.35	A				–	–				

[a] Tukey grouping. Groups with common letters are not significantly different.

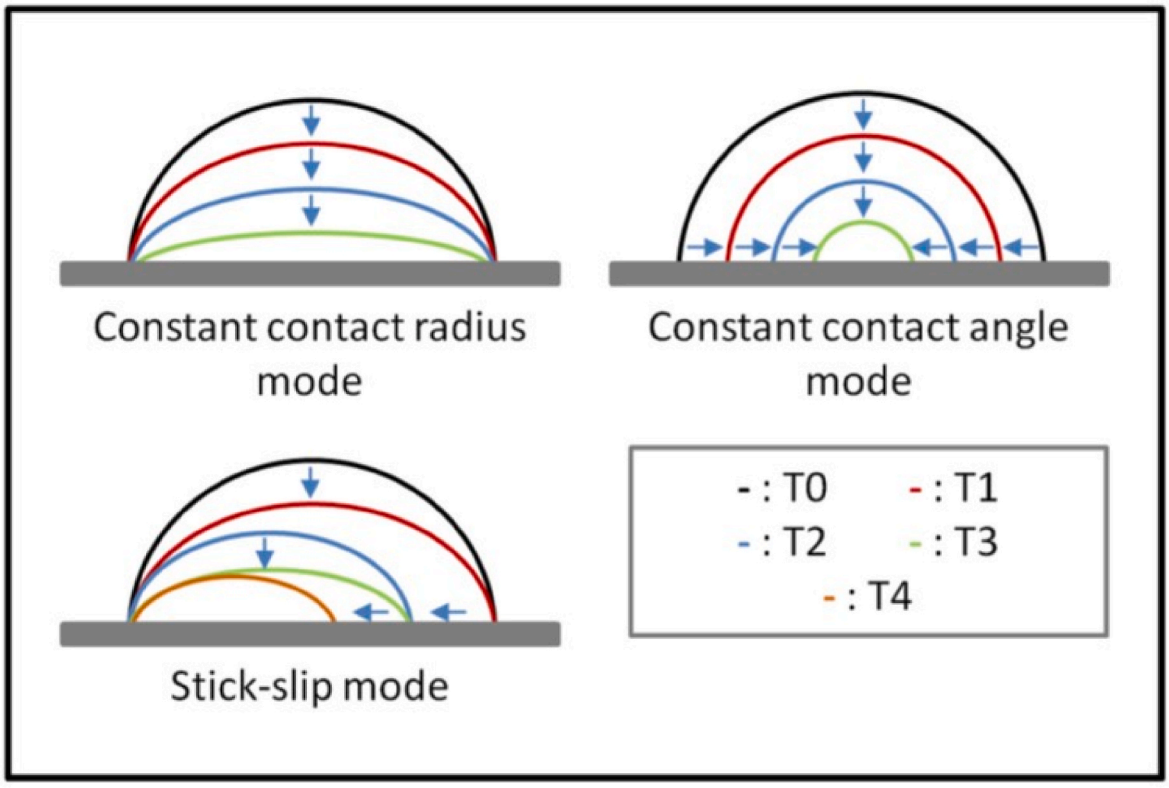

Fig. 4. Various evaporation modes of droplets settled on a surface. T0 to T4 = different times of drying.

angle and the droplet diameter can vary. This is for example, the case of the "stick-slip" mode, in which the contact line undergoes successive jumps between pinning sites (the contact line recedes). The evaporation mode is largely controlled by the material roughness (Ta et al., 2016; Zhang et al., 2018) and physicochemical property (Burkhart et al., 2017). First, under the experimental conditions of this study, the material topography does not seem to affect the drying mode or the organization of the final deposit after drying. This result is consistent with previous work performed in the laboratory, which failed to demonstrate a preferential adhesion of spores at small surface defects, such as grain boundaries (data not shown). Conversely, our results confirmed that the CCR mode (pinned droplets) would be favored during drying on hydrophilic surfaces, while highly hydrophobic materials would promote the CCA mode. Regarding the role of materials, the results obtained in this study confirmed the major influence of hydrophilic/hydrophobic properties of the material on the deposit pattern, consistent with results presented in the literature (Burkhart et al., 2017; Patil et al., 2016). While a peripheral ring was clearly observed in the CCR mode (on glass and stainless steel), the CCA mode (on PP) resulted rather in the formation of a more or less centralized cluster of particles.

On the other hand, contrary to what has been reported in the literature, it was not possible to clearly demonstrate the phenomenon of "self-pinning" of the contact line promoted by the presence of particles within the droplets (Orejon et al., 2011) except perhaps at the level of the droplet shape at the time of deposition. Indeed, the presence of spores limited the spreading of the droplets on the different materials, which resulted in lower contact angles with the water. Conversely, the properties of the spores affected, but to a small extent, the drying kinetics and the pining of the droplets and the subsequent formation of the peripheral ring was more marked when they contained hydrophilic spores.

All these phenomena are of course directly related to the movement of particles during the drying process. Indeed, during the drying process, the particles are subjected to water flows within the droplets. As the temperature at the surface of the droplet is not uniformly distributed, the evaporation flux increases along the surface from the top to the edge of the droplet, resulting in an outward flow to replenish the evaporation loss (Zhong et al., 2015). Depending on the nature of the particles and the fluid as well as the environmental conditions, it is thus possible to observe in particular a radial capillary flow that is sometimes accompanied by a recirculation phenomenon, known as the Marangoni recirculation loop (Parsa et al., 2018). The particles subjected to these flow regimes are thus driven outward. This outward migration is clearly observed in this study with *Bacillus* spores on both materials, mainly when both surfaces in contact are highly hydrophilic (Bs PY79 on hydrophilic glass) and this movement was observed throughout the drying period. On the other hand, for hydrophobic spores, their observation during drying clearly revealed two concomitant phenomena. Firstly, a strong interaction between spores and materials prevented them from migrating to the edge of the droplet and resulted at least in part in the numerous spores and spore clusters across the whole surface initially covered by the droplet. Since hydrophobic *Bacillus* spores are known to adhere strongly to all types of materials (Faille et al., 2010), this would explain why many Bc 98/4 spores and spore clusters remain stationary during drying. Secondly, an outward migration of the non-adherent spores resulted in a diffuse peripheral ring.

Given the different deposit patterns observed, but also the different properties of the surfaces in contact (materials vs. spores), the effectiveness of rinsing or cleaning procedures can be expected to be more or less pronounced. However, as far as is known, none of the studies on bioaerosols available in the literature have focused on this point, despite its probable importance in the control of surface hygiene in the food industry and any other sector concerned by these aerosols. A first striking result is the very high resistance of the spore deposits to a rinsing procedure (mechanical detachment due to the water flow) with frequently fewer than 50% spores being released. An earlier study that involved spores adhered to coupons immersed in a spore suspension also showed strong resistance of adhering spores to a rinsing procedure at

500 Pa (Faille et al., 2013). However, between 50 and 90% of the spores were released (thus more than the percentages obtained for droplets), suggesting that the deposits formed by droplet drying are particularly resistant to detachment by a water flow. Furthermore, in the present study, the deposit formed by the highly hydrophilic Bs PY79 spores were significantly less resistant to detachment than the other four, moderately to strongly hydrophobic spores, except perhaps on SS-2B. This is probably because the outer ring contained most of the spores in the final deposit in the case of Bs PY79. Indeed, whatever their surface properties, spores in the outer ring were more sensitive to mechanical forces than the spores isolated or in clusters on the rest of the surface, as shown by the microscopic observations of the drops that underwent the rinsing procedure. This low resistance of the outer ring resulting from the accumulation of spores at the periphery of the drop is likely not due to any specific affinity between the spores and the material (adhesion) or between the spores (cohesion). Another explanation would be that, in the case of a thick ring formed by several layers of spores, this ring could be more affected by the shear forces, thus facilitating its detachment. Indeed, a similar phenomenon was also observed for the thick spore clusters formed by Bc 98/4 and Bc D6. This observation is consistent with other observations reported in the literature, whether on spore clusters (Al Saabi et al., 2021) or on *P. fluorescens* biofilms (Benezech and Faille, 2018) which were rapidly removed during cleaning procedures.

Additional experiments were performed to investigate the resistance to cleaning of the deposits and therefore the consequences of bioaerosols settled on a material in order to forecast surface hygiene. As one may have expected, the cleaning procedure was much more effective than the rinsing procedure, with, in most cases, less than 10% of residual adherent spores. The hydrophilic/hydrophobic character of the surface in contact seems to be the major parameter affecting the ease of detachment, as previously reported (Faille et al., 2002). Indeed, whatever the strain, lower numbers of residual spores were obtained on glass and it was difficult to discriminate between the other three materials. The same trend was observed for the hydrophilic/hydrophobic character of the spores, the very hydrophilic spores of Bs PY79 being much more easily removed than the other spores, whether more or less hydrophobic, which is consistent with the work mentioned above (Faille et al., 2013). The observation of images of the deposits taken before and after the cleaning procedure confirmed that the pattern of the deposit also affected the ease of removal. As for the rinsing procedure, the ring was partially or totally removed, due to its fragility with respect to the detachment procedure.

5. Conclusion

Depending on the properties of materials and spores suspended in aerosols, different phenomena occur during the drying of droplets on a surface, resulting in the formation of deposits with different patterns. A major element is the rapid interaction between hydrophobic spores and surfaces, which counteracts their migration towards the periphery and thus limits the ring formation that is observed in most cases. Moreover, besides the hydrophilic/hydrophobic properties of the surfaces in contact (materials vs spores), the organization of the deposits also affects their resistance to rinsing and/or cleaning procedures. In particular, the spores in the coffee-ring (hydrophilic material) are more easily removed than the spores present on the inner surface, whether they are isolated or in clusters. In any case, these droplets dried for 1 h are already very resistant to a CIP procedure, especially on hydrophobic materials, but also on stainless steel, and this resistance will certainly be further increased when the surfaces are subjected to a long period of drying. As stainless steels and polymers are frequently encountered in food processing lines, including in packaging, the persistence of these complex deposits requires increased vigilance regarding the effectiveness of disinfection procedures in aerosols affected environments.

Credit author statement

Maureen Deleplace: Investigation; Methodology. Heni Dallagi: Investigation; Methodology. Thomas Dubois: Investigation; Methodology. Elodie Richard: Investigation; Methodology. Anna Ipatova: Investigation. Thierry Benezech: Funding acquisition; Validation. Christine Faille: Supervision; Conceptualization; Validation; Writing.

Declaration of competing interest

The authors have no conflict of interest to declare.

Acknowledgements

The authors are grateful to Christelle Lemy and Andrea Huette from UMET, for their valuable technical assistance.

Appendix A. Supplementary data

Supplementary data to this article can be found online at https://doi.org/10.1016/j.jfoodeng.2021.110873.

Funding

This work was supported by the ANR (Agence Nationale de la Recherche) for funding the FEFS project (contract number ANR-18-CE21-0010) and the Region Hauts-de-France for funding the Interreg Veg-I-Tec project (Programme Interreg V France-Wallonia-Flanders, GoToS3).

References

Al Saabi, A., Dallagi, H., Aloui, F., Faille, C., Rauwel, G., Wauquier, L., Bouvier, L., Bénézech, T., 2021. Removal of Bacillus spores from stainless steel pipes by flow foam: effect of the foam quality and velocity. J. Food Eng. 289 https://doi.org/10.1016/j.jfoodeng.2020.110273.

Baughman, K.F., Maier, R.M., Norris, T.A., Beam, B.M., Mudalige, A., Pemberton, J.E., Curry, J.E., 2010. Evaporative deposition patterns of bacteria from a sessile drop: effect of changes in surface wettability due to exposure to a laboratory atmosphere. Langmuir 26, 7293–7298. https://doi.org/10.1021/la100932k.

Benezech, T., Faille, C., 2018. Two-phase kinetics of biofilm removal during CIP. Respective roles of mechanical and chemical effects on the detachment of single cells vs cell clusters from a Pseudomonas fluorescens biofilm. J. Food Eng. 219, 121–128. https://doi.org/10.1016/j.jfoodeng.2017.09.013.

Burkhart, C.T., Maki, K.L., Schertzer, M.J., 2017. Effects of interface velocity, diffusion rate, and radial velocity on colloidal deposition patterns left by evaporating droplets. J. Heat Tran. 139, 1–9. https://doi.org/10.1115/1.4036681.

Coughlan, L.M., Cotter, P.D., Hill, C., Alvarez-Ordóñez, A., 2016. New weapons to fight old enemies: novel strategies for the (bio)control of bacterial biofilms in the food industry. Front. Microbiol. 7, 1–21. https://doi.org/10.3389/fmicb.2016.01641.

Delplace, F., 2018. Fluids flow stability in ducts of arbitrary cross-section. J. Mod. Appl. Phys. 2, 10–15.

Devlin, N., Loehr, K., Harris, M., 2015. The separation of two different sized particles in an evaporating droplet. AIChE J. 61, 3547–3556. https://doi.org/10.1002/aic.

Dubois, T., Krzewinski, F., Yamakawa, N., Lemy, C., Hamiot, A., Brunet, L., Lacoste, A.S., Knirel, Y., Guerardel, Y., Faille, C., 2020. The sps genes encode an original legionaminic acid pathway required for crust assembly in bacillus subtilis. mBio 11, 1–17. https://doi.org/10.1128/mBio.01153-20.

Eduard, W., Heederik, D., Duchaine, C., Green, B.J., 2012. Bioaerosol exposure assessment in the workplace: the past, present and recent advances. J. Environ. Monit. 14, 334–339. https://doi.org/10.1039/c2em10717a.

Faille, C., Bénézech, T., Blel, W., Ronse, A., Ronse, G., Clarisse, M., Slomianny, C., 2013. Role of mechanical vs. chemical action in the removal of adherent Bacillus spores during CIP procedures. Food Microbiol. 33, 149–157. https://doi.org/10.1016/j.fm.2012.09.010.

Faille, C., Bénézech, T., Midelet-Bourdin, G., Lequette, Y., Clarisse, M.A., Ronse, G., Ronse, A., Slomianny, C., 2014. Sporulation of Bacillus spp. within biofilms: a potential source of contamination in food processing environments. Food Microbiol. 40, 64–74. https://doi.org/10.1016/j.fm.2013.12.004.

Faille, C., Billet, E., 2020. The aerosolisation phenomenon. Aerosol droplets and cross-contamination risks in the food industry. New Food 3, 51–54.

Faille, C., Jullien, C., Fontaine, F., Bellon-Fontaine, M.N., Slomianny, C., Benezech, T., 2002. Adhesion of Bacillus spores and Escherichia coli cells to inert surfaces: role of surface hydrophobicity. Can. J. Microbiol. 48, 728–738. https://doi.org/10.1139/w02-063.

Faille, C., Lemy, C., Allion-maurer, A., Zoueshtiagh, F., 2019. Evaluation of the hydrophobic properties of latex microspheres and Bacillus spores. In fl uence of the particle size on the data obtained by the MATH method (microbial adhesion to hydrocarbons). Colloids Surf. B Biointerfaces 182.

Faille, C., Lequette, Y., Ronse, A., Slomianny, C., Garénaux, E., Guerardel, Y., 2010. Morphology and physico-chemical properties of Bacillus spores surrounded or not with an exosporium. Consequences on their ability to adhere to stainless steel. Int. J. Food Microbiol. 143, 125–135. https://doi.org/10.1016/j.ijfoodmicro.2010.07.038.

Holah, J., 2018. Cleaning and Disinfection Objectives, Reference Module in Food Science. Elsevier. https://doi.org/10.1016/b978-0-08-100596-5.21203-1.

Jullien, C., Benezech, T., Gentil, C.L., Boulange-Petermann, L., Dubois, P.E., Tissier, J.P., Traisnel, M., Faille, C., 2008. Physico-chemical and hygienic property modifications of stainless steel surfaces induced by conditioning with food and detergent. Biofouling 24, 163–172. https://doi.org/10.1080/08927010801958960.

Kuda, T., Shibata, G., Takahashi, H., Kimura, B., 2015. Effect of quantity of food residues on resistance to desiccation of food-related pathogens adhered to a stainless steel surface. Food Microbiol. 46, 234–238. https://doi.org/10.1016/j.fm.2014.08.014.

Merrill, L., Dunbar, J., Richardson, J., Kuske, C.R., 2006. Composition of Bacillus species in aerosols from 11 U.S. cities. J. Forensic Sci. 51, 559–565. https://doi.org/10.1111/j.1556-4029.2006.00132.x.

Orejon, D., Sefiane, K., Shanahan, M.E.R., 2011. Stick-slip of evaporating droplets: substrate hydrophobicity and nanoparticle concentration. Langmuir 27, 12834–12843. https://doi.org/10.1021/la2026736.

Parsa, M., Harmand, S., Sefiane, K., 2018. Mechanisms of pattern formation from dried sessile drops. Adv. Colloid Interface Sci. 254, 22–47. https://doi.org/10.1016/j.cis.2018.03.007.

Patil, N.D., Bange, P.G., Bhardwaj, R., Sharma, A., 2016. Effects of substrate heating and wettability on evaporation dynamics and deposition patterns for a sessile water droplet containing colloidal particles. Langmuir 32, 11958–11972. https://doi.org/10.1021/acs.langmuir.6b02769.

Radeck, J., Kraft, K., Bartels, J., Cikovic, T., Dürr, F., Emenegger, J., Kelterborn, S., Sauer, C., Fritz, G., Gebhard, S., Mascher, T., 2013. The Bacillus BioBrick Box: generation and evaluation of essential genetic building blocks for standardized work with Bacillus subtilis. J. Biol. Eng. 7 https://doi.org/10.1186/1754-1611-7-29.

Richard, E., Dubois, T., Allion-Maurer, A., Jha, P.K., Faille, C., 2020. Hydrophobicity of abiotic surfaces governs droplets deposition and evaporation patterns. Food Microbiol. 91, 103538 https://doi.org/10.1016/j.fm.2020.103538.

Spurlock, A.T., Zottola, E.A., 1991. The survival of Listeria monocytogenes in aerosols. J. Food Protect. 54, 910–912. https://doi.org/10.4315/0362-028x-54.12.910.

Susarrey-Arce, A., Marin, A., Massey, A., Oknianska, A., Díaz-Fernandez, Y., Hernández-Sánchez, J.F., Griffiths, E., Gardeniers, J.G.E., Snoeijer, J.H., Lohse, D., Raval, R., 2016. Pattern formation by Staphylococcus epidermidis via droplet evaporation on micropillars arrays at a surface. Langmuir 32, 7159–7169. https://doi.org/10.1021/acs.langmuir.6b01658.

Ta, V.D., Dunn, A., Wasley, T.J., Li, J., Kay, R.W., Stringer, J., Smith, P.J., Esenturk, E., Connaughton, C., Shephard, J.D., 2016. Laser textured superhydrophobic surfaces and their applications for homogeneous spot deposition. Appl. Surf. Sci. 365, 153–159. https://doi.org/10.1016/j.apsusc.2016.01.019.

Theisinger, S.M., Smidt, O. de, 2017. Bioaerosols in the food and beverage industry. Ideas appl. Towar. Sample Prep. Food Beverage Anal. https://doi.org/10.5772/intechopen.69978.

Yunker, P.J., Still, T., Lohr, M.A., Yodh, A.G., 2011. Suppression of the coffee-ring effect by shape-dependent capillary interactions. Nature 476, 308–311. https://doi.org/10.1038/nature10344.

Zhang, Y., Chen, X., Liu, F., Li, L., Dai, J., Liu, T., 2018. Enhanced coffee-ring effect via substrate roughness in evaporation of colloidal droplets. Adv. Condens. Matter Phys. https://doi.org/10.1155/2018/9795654, 2018.

Zhong, X., Crivoi, A., Duan, F., 2015. Sessile nanofluid droplet drying. Adv. Colloid Interface Sci. 217, 13–30. https://doi.org/10.1016/j.cis.2014.12.003.